A General Class of Passive Macromodels for Lossy Multiconductor Transmission Lines

Anestis Dounavis, *Student Member, IEEE,* Ramachandra Achar, *Member, IEEE*, and Michel Nakhla, *Fellow, IEEE*

***Abstract*—This paper presents a general class of passive macromodeling algorithm for multiport distributed interconnects. A new theorem is described that specifies sufficient conditions for matrix-rational approximation of exponential functions in order to generate a passive macromodel. A proof is given showing that the currently existing passive matrix-rational approximation of exponential functions is a subclass of the generic approach presented in this paper. In addition, a technique to obtain a compact passive macromodel with predetermined coefficients, based on near-optimal approximation, is presented. The proposed model can be easily incorporated with recently developed passive model-reduction techniques.**

***Index Terms*—Circuit simulation, distributed networks, high-speed interconnects, transmission lines.**

I. Introduction

THE phenomenal growth in density, operating speeds, and complexity of modern integrated circuits has made interconnect analysis a requirement for all state-of-the-art circuit simulators. Interconnect effects such as ringing, signal delay, distortion, attenuation, and crosstalk can severely degrade signal integrity. Interconnections can be from various levels of design hierarchy, such as on-chip, packaging structures, multichip modules (MCMs), printed circuit boards (PCBs), and backplanes. As the frequency of operation increases, the length of the interconnects become a significant fraction of the operating wavelength, and conventional lumped models become inadequate in describing the interconnect performance and transmission-line models become necessary. Skin and proximity effects also become prominent at high frequencies and distributed models with frequency-dependent parameters may be needed [1]–[21].

The major difficulty usually encountered while linking the distributed transmission-line models and nonlinear simulators is the problem of mixed frequency/time. This is because distributed elements are usually characterized in the frequency domain where as nonlinear components such as drivers and receivers are represented only in time domain. Several publications can be found in the literature that address this issue [4]–[12], [16]–[20]. Approaches based on conventional lumped segmentation of transmission lines provide a brute-force solution to the problem of mixed frequency/time simulation. However, these methods lead to large circuit matrices, rendering the simulation inefficient. A passive transmission-line macromodel based on a closed-form matrix-rational approximation of an exponential function was proposed in [9]–[11]. The method uses the predetermined constants given by the closed-form matrix-rational approximation and the per-unit-length parameters to obtain ordinary differential equations analytically.

In this paper, a general class of passive macromodeling algorithm for multiport distributed interconnects is presented. The proposed approach is based on matrix-rational approximation of exponential functions describing Telegrapher's equations. A new theorem is described, which specifies the necessary conditions for any matrix-rational approximation of exponential functions so as to generate a passive macromodel. Also, a proof is given showing that the currently existing passive matrix-rational approximation techniques [9]–[11] for exponential functions are a subclass of the generic approach presented in this paper.

In addition, a technique is described to obtain a near-optimal rational approximation for exponential functions. Near-optimal approximations (such as minimax approximations) are able to distribute the error more evenly in a given interval and, thus, are able to achieve higher accuracy for equal orders when compared to Padé approximations. The objective is to predetermine the coefficients of optimal rational approximations for exponential functions, while ensuring the coefficients do not violate passivity when used to model transmission lines. These coefficients can be computed *a priori* and are stored. This enables the development of the transmission-line macromodel to be formulated analytically in terms of known (stored) constants and given per-unit-length parameters. Also, the proposed model can be easily incorporated with the recently developed passive model-reduction techniques [11], [19], [20]. Numerical examples are presented to demonstrate the validity and efficiency of the proposed method.

The organization of this paper is as follows. A brief review of transmission-line equations and macromodeling is given in Section II. Development of the proposed generic distributed interconnect model and a new theorem, as well as its proof, is given in Section III. A new technique to obtain near-optimal approximation for exponential functions is described in Section IV. Section V provides a brief outline of the development of the time-domain macromodel. Sections VI and VII provide the numerical results and conclusions, respectively.

II. Review of Transmission-Line Macromodeling

Distributed interconnects are described by a set of partial differential equations known as Telegrapher's equations as follows:

$$\frac{\partial}{\partial x}\boldsymbol{v}(x,t) = -\boldsymbol{R}\boldsymbol{i}(x,t) - \boldsymbol{L}\frac{\partial}{\partial t}\boldsymbol{i}(x,t)$$
$$\frac{\partial}{\partial x}\boldsymbol{i}(x,t) = -\boldsymbol{G}\boldsymbol{v}(x,t) - \boldsymbol{C}\frac{\partial}{\partial t}\boldsymbol{v}(x,t) \qquad (1)$$

Manuscript received January 15, 2001.

The authors are with the Department of Electronics, Carleton University, Ottawa, ON, Canada K1S 5B6.

Publisher Item Identifier S 0018-9480(01)08690-2.

where $\boldsymbol{R} \in \Re^{\psi\times\psi}$, $\boldsymbol{L} \in \Re^{\psi\times\psi}$, $\boldsymbol{C} \in \Re^{\psi\times\psi}$, and $\boldsymbol{G} \in \Re^{\psi\times\psi}$ are the per-unit-length parameters of the transmission line and are symmetric nonnegative definite [3], [6], $\boldsymbol{V}(x, t) \in \Re^{\psi}$ and $\boldsymbol{I}(x, t) \in \Re^{\psi}$ represent the voltage and current vectors as a function of position x and time t, and ψ is the number coupled lines. Equation (1) can be written in the Laplace domain as an exponential matrix function as

$$\begin{bmatrix} \boldsymbol{V}(d, s) \\ \boldsymbol{I}(d, s) \end{bmatrix} = e^{\boldsymbol{Z}} \begin{bmatrix} \boldsymbol{V}(0, s) \\ \boldsymbol{I}(0, s) \end{bmatrix} \tag{2}$$

where

$$\boldsymbol{Z} = (\boldsymbol{D} + s\boldsymbol{E})d \quad \boldsymbol{D} = \begin{bmatrix} \boldsymbol{0} & -\boldsymbol{R} \\ -\boldsymbol{G} & \boldsymbol{0} \end{bmatrix} \quad \boldsymbol{E} = \begin{bmatrix} \boldsymbol{0} & -\boldsymbol{L} \\ -\boldsymbol{C} & \boldsymbol{0} \end{bmatrix} \tag{3}$$

$\boldsymbol{V}$, $\boldsymbol{I}$ represent the Laplace-domain terminal voltage and current vectors of the multiconductor transmission line, and d is the length of the line.

Equation (2) does not have a direct representation in the time domain, which makes it difficult to interface with nonlinear simulators. Several publications can be found in the literature to address this issue [4]–[12]. In [9]–[11], a closed-form passive Padé model based on matrix-rational approximation is suggested for modeling distributed transmission lines, which provides an efficient means to address the issue of mixed frequency/time simulation. The objective of this paper is to present a general class of algorithm that can ensure passivity of any type of matrix-rational approximation of exponential functions. Also, we will show that the technique provided in [9]–[11] is a subset of the general class of passive matrix-rational approximation presented in this paper.

III. Development of the Proposed Passive Distributed Interconnect Macromodel

A scalar exponential function can be approximated as a rational function as

$$e^s \approx \frac{Q_N(s)}{P_M(s)} = \frac{\sum_{i=0}^{N} q_i s^i}{\sum_{i=0}^{M} p_i s^i} \tag{4}$$

where $s = j\omega$. If the scalar s is replaced by the matrix $\boldsymbol{Z}$, then a rational matrix is obtained, which can be used to model transmission lines described by (2) as

$$\boldsymbol{P}_M(\boldsymbol{Z})e^{\boldsymbol{Z}} = \boldsymbol{Q}_N(\boldsymbol{Z}). \tag{5}$$

where $\boldsymbol{P}_M(\boldsymbol{Z})$, $\boldsymbol{Q}_N(\boldsymbol{Z})$ are polynomial matrices expressed as

$$\boldsymbol{Q}_N(\boldsymbol{Z}) = \sum_{i=0}^{N} q_i \boldsymbol{Z}^i \quad \boldsymbol{P}_M(\boldsymbol{Z}) = \sum_{i=0}^{M} p_i \boldsymbol{Z}^i. \tag{6}$$

Once the exponential matrix of (2) is represented as rational functions, ordinary differential equations can be obtained. The formulation of these equations are obtained analytically in terms of predetermined constants (i.e., p_i, q_i) and the $\boldsymbol{RLGC}$ parameters. In the following section, we focus on the passivity issues of the proposed macromodel.

A. Passivity Considerations

A linear n-port network with an admittance matrix $\boldsymbol{Y}(s)$ is said to be passive, if and only if [22]: 1) $\boldsymbol{Y}(s^*) = \boldsymbol{Y}^*(s)$ for all s, where $*$ is the complex conjugate operator and 2) $\boldsymbol{Y}(s)$ is a positive-real matrix. That is the product $\boldsymbol{z}^{*t}[\boldsymbol{Y}^t(s^*)+\boldsymbol{Y}(s)]\boldsymbol{z} \geq 0$ for all possible values of s satisfying $\mathrm{Re}(s) > 0$ and for any arbitrary value of $\boldsymbol{z}$.

The first condition implies that the coefficients of the rational function matrix generated by the proposed macromodel must be real. The second condition implies, that $\boldsymbol{Y}(s)$ must be a positive-real matrix for all $\mathrm{Re}(s) > 0$ since $\mathrm{Real}(\boldsymbol{Y}(s)) = 1/2[\boldsymbol{Y}^t(s^*) + \boldsymbol{Y}(s)]$. The coefficients generated by (5) are real values, therefore, the first condition of the passivity definition is always satisfied. The task that remains is to ensure that the rational approximation satisfies the second condition. For this purpose, we present the following new theorem.

Theorem 1: Let the rational function approximation of e^s be

$$e^s \approx \frac{Q_N(s)}{Q_N(-s)} = \frac{\sum_{i=0}^{N} q_i s^i}{\sum_{i=0}^{N} q_i (-s)^i} \tag{7}$$

where the polynomial $Q_N(s)$ is strictly Hurwitz. *If the above conditions are satisfied, then the rational matrix obtained by replacing the scalar s with the matrix $\boldsymbol{Z}$ of* (3) *results in a passive transmission-line macromodel.*

The form of the resulting matrix-rational approximation can be written as

$$\boldsymbol{Q}_N(-\boldsymbol{Z}) \begin{bmatrix} \boldsymbol{V}(d, s) \\ \boldsymbol{I}(d, s) \end{bmatrix} \approx \boldsymbol{Q}_N(\boldsymbol{Z}) \begin{bmatrix} \boldsymbol{V}(0, s) \\ \boldsymbol{I}(0, s) \end{bmatrix} \tag{8}$$

or

$$\begin{bmatrix} \boldsymbol{Q}_{N_{11}} & \boldsymbol{Q}_{N_{12}} \\ \boldsymbol{Q}_{N_{21}} & \boldsymbol{Q}_{N_{22}} \end{bmatrix} \begin{bmatrix} \boldsymbol{V}(d, s) \\ \boldsymbol{I}(d, s) \end{bmatrix} \approx \begin{bmatrix} \boldsymbol{Q}_{N_{11}} & -\boldsymbol{Q}_{N_{12}} \\ -\boldsymbol{Q}_{N_{21}} & \boldsymbol{Q}_{N_{22}} \end{bmatrix} \begin{bmatrix} \boldsymbol{V}(0, s) \\ \boldsymbol{I}(0, s) \end{bmatrix} \tag{9}$$

where

$$\boldsymbol{Q}_N(\boldsymbol{Z}) = \sum_{i=0}^{N} q_i \boldsymbol{Z}^i \tag{10a}$$

$$\boldsymbol{Q}_{N_{11}} = \sum_{i=0}^{N} q_i \left[\frac{1}{2}(1 + (-1)^i)(\boldsymbol{ab})^{i/2}\right] \tag{10b}$$

$$\boldsymbol{Q}_{N_{12}} = \sum_{i=0}^{N} q_i \left[\frac{1}{2}(1 - (-1)^i)(\boldsymbol{ab})^{(i-1)/2}\boldsymbol{a}\right] \tag{10c}$$

$$\boldsymbol{Q}_{N_{21}} = \sum_{i=0}^{N} q_i \left[\frac{1}{2}(1 - (-1)^i)(\boldsymbol{ba})^{(i-1)/2}\boldsymbol{b}\right] \tag{10d}$$

$$\boldsymbol{Q}_{N_{22}} = \sum_{i=0}^{N} q_i \left[\frac{1}{2}(1 + (-1)^i)(\boldsymbol{ba})^{i/2}\right] \tag{10e}$$

and $\boldsymbol{a} = \boldsymbol{R} + s\boldsymbol{L}$; $\boldsymbol{b} = \boldsymbol{G} + s\boldsymbol{C}$.

The conditions on the scalar rational approximation represented by (7) in Theorem 1 essentially means the following.

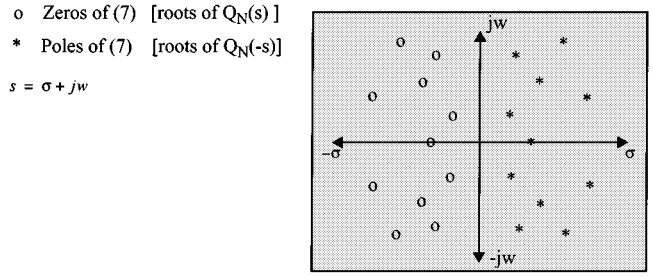

Fig. 1. Pole-zero distribution requirement for scalar rational approximation of (7) in Theorem 1.

A strict Hurwitz polynomial [in this case, $Q_N(s)$] has its roots only in the left half-plane. Hence, the zeros of scalar rational approximation (7) are strictly on left half-plane. The poles of the rational approximation (7), which is given by the roots of $Q_N(-s)$, will all be on the right half-plane and are mirror images of zeros of (7). A graphical description of the pole-zero distribution requirement for the scalar rational approximation represented by (7) in Theorem 1 is shown in Fig. 1.

Proof of Theorem 1: The passivity proof associated with the above theorem is provided in terms of the Y-parameter form of (9). Using (9), we can write

$$\begin{bmatrix} \boldsymbol{I}_{(0,s)} \\ -\boldsymbol{I}_{(d,s)} \end{bmatrix} = \begin{bmatrix} \boldsymbol{Y}_{11} & \boldsymbol{Y}_{12} \\ \boldsymbol{Y}_{21} & \boldsymbol{Y}_{22} \end{bmatrix} \begin{bmatrix} \boldsymbol{V}_{(0,s)} \\ \boldsymbol{V}_{(d,s)} \end{bmatrix} \tag{11}$$

where

$$\begin{bmatrix} \boldsymbol{Y}_{11} & \boldsymbol{Y}_{12} \\ \boldsymbol{Y}_{21} & \boldsymbol{Y}_{22} \end{bmatrix} = \boldsymbol{\Psi}_1 + \Psi_2 \tag{12}$$

and

$$\boldsymbol{\Psi}_1 = \begin{bmatrix} \frac{1}{2}\left[\boldsymbol{Q}_{N_{12}}\right]^{-1}\boldsymbol{Q}_{N_{11}} & -\frac{1}{2}\left[\boldsymbol{Q}_{N_{12}}\right]^{-1}\boldsymbol{Q}_{N_{11}} \\ -\frac{1}{2}\left[\boldsymbol{Q}_{N_{12}}\right]^{-1}\boldsymbol{Q}_{N_{11}} & \frac{1}{2}\left[\boldsymbol{Q}_{N_{12}}\right]^{-1}\boldsymbol{Q}_{N_{11}} \end{bmatrix} \tag{13a}$$

$$\boldsymbol{\Psi}_2 = \begin{bmatrix} \frac{1}{2}\left[\boldsymbol{Q}_{N_{22}}\right]^{-1}\boldsymbol{Q}_{N_{21}} & \frac{1}{2}\left[\boldsymbol{Q}_{N_{22}}\right]^{-1}\boldsymbol{Q}_{N_{21}} \\ \frac{1}{2}\left[\boldsymbol{Q}_{N_{22}}\right]^{-1}\boldsymbol{Q}_{N_{21}} & \frac{1}{2}\left[\boldsymbol{Q}_{N_{22}}\right]^{-1}\boldsymbol{Q}_{N_{21}} \end{bmatrix}. \tag{13b}$$

To prove that $\boldsymbol{\Psi}_1$ and $\boldsymbol{\Psi}_2$ are positive real, the matrices are written in terms of congruent transforms as

$$\begin{aligned} \boldsymbol{\Psi_1} &= \boldsymbol{W}_\alpha^{\boldsymbol{t}} \operatorname{diag}\left(\frac{1}{2}\boldsymbol{H}_a, \boldsymbol{0}\right) \boldsymbol{W}_\alpha \\ \boldsymbol{\Psi_2} &= \boldsymbol{W}_\beta^{\boldsymbol{t}} \operatorname{diag}\left(\frac{1}{2}\boldsymbol{H}_b, \boldsymbol{0}\right) \boldsymbol{W}_\beta \end{aligned} \tag{14}$$

where

$$\begin{aligned} \boldsymbol{W}_\alpha &= \begin{bmatrix} \boldsymbol{U} & -\boldsymbol{U} \\ \boldsymbol{0} & \boldsymbol{U} \end{bmatrix} \\ \boldsymbol{W}_\beta &= \begin{bmatrix} \boldsymbol{U} & \boldsymbol{U} \\ \boldsymbol{0} & \boldsymbol{U} \end{bmatrix}; \\ \boldsymbol{H}_a &= \left[\boldsymbol{Q}_{N_{12}}\right]^{-1}\boldsymbol{Q}_{N_{11}} \\ \boldsymbol{H}_b &= \left[\boldsymbol{Q}_{N_{22}}\right]^{-1}\boldsymbol{Q}_{N_{21}} \end{aligned} \tag{15}$$

and $\boldsymbol{U}$ is the unity matrix.

If the matrices $\operatorname{diag}(1/2\boldsymbol{H}_a, \boldsymbol{0})$ and $\operatorname{diag}(1/2\boldsymbol{H}_b, \boldsymbol{0})$ are positive real, then $\boldsymbol{\Psi_1}$ and $\boldsymbol{\Psi_2}$ are positive real since they are expressed in terms of congruence transformations of positive-real matrices. Thus, to prove the passivity of the macromodel, the rational matrices $\boldsymbol{H}_a$ and $\boldsymbol{H}_b$ must be shown to be positive real. For this purpose, we utilize the condition that the polynomial $Q_N(s)$ of (7) is a strict Hurwitz polynomial. To identify if a polynomial is a strict Hurwitz polynomial, it is separated into even and odd parts as [23]

$$\begin{aligned} Q_N(s) &= \sum_{i=0}^{N} q_i s^i \\ Q_{\mathrm{EV}}(s) &= \sum_{i=0}^{N} q_i \left[\frac{1}{2}\left(1+(-1)^i\right)s^i\right] \\ Q_{\mathrm{ODD}}(s) &= \sum_{i=0}^{N} q_i \left[\frac{1}{2}\left(1-(-1)^i\right)s^i\right] \end{aligned} \tag{16}$$

where $Q_{\mathrm{EV}}(s)$ and $Q_{\mathrm{ODD}}(s)$ represent the even and odd functions of $Q_N(s)$, respectively. The rational function formed from the even and odd polynomials can be expressed as a continued fraction expansion. For example, *if the order of the polynomial is even*, the continued fraction expansion becomes

$$\frac{Q_{\mathrm{EV}}(s)}{Q_{\mathrm{ODD}}(s)} = \kappa_N s + \cfrac{1}{\kappa_{N-1}s + \cfrac{1}{\kappa_{N-2}s + \cdots \\ \ddots \\ \kappa_1 s}}. \tag{17}$$

The necessary and sufficient conditions for $Q_N(s)$ to be a strict Hurwitz polynomial are the coefficients κ_i for $i = 1, 2, \ldots, N$ must be strictly positive. This is stated in Lemma 1.

Lemma 1:

- If $Q_N(s)$ is a strict Hurwitz polynomial, then the rational function created using the even and odd polynomials of (17) is an odd positive-real rational function [23].

Also, the following facts are used to prove that $\boldsymbol{H}_a$ and $\boldsymbol{H}_b$ are positive real.

Lemma 2:

- The sum of two positive-real matrices of similar dimensions is positive real [24].

Lemma 3:

- The inverse of a positive-real matrix (if the inverse exists), is positive real [24].

It should be noted that $Q_{\mathrm{EV}}(s)$ and $Q_{\mathrm{ODD}}(s)$ of (16) are very similar in form to $\boldsymbol{Q}_{N_{11}}, \boldsymbol{Q}_{N_{12}}, \boldsymbol{Q}_{N_{21}}$, and $\boldsymbol{Q}_{N_{22}}$ of (10b)–(10e). In fact, a relationship exists between the two forms, and we will use this relation to prove that $\boldsymbol{H}_a$ and $\boldsymbol{H}_b$ are positive-real functions. Let the rational-function formed by $Q_{\mathrm{EV}}(s)$ and $Q_{\mathrm{ODD}}(s)$ be expressed as a continued fraction

$$\frac{Q_{\mathrm{EV}}(s)}{Q_{\mathrm{ODD}}(s)} = \kappa_N s + \cfrac{1}{\kappa_{N-1}s + \cfrac{1}{\kappa_{N-2}s + \cdots \\ \ddots \\ \kappa_1 s}}, \qquad \text{if } N = \text{Even}$$

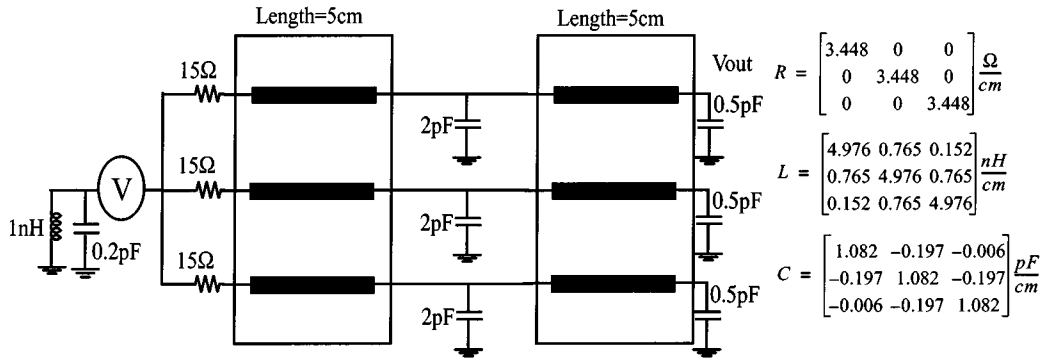

Fig. 2. Coupled interconnect system.

$$\frac{Q_{\mathrm{EV}}(s)}{Q_{\mathrm{ODD}}(s)} = \cfrac{1}{\kappa_N s + \cfrac{1}{\kappa_{N-1}s + \cfrac{1}{\kappa_{N-2}s + \cdots}}} \qquad \text{if } N = \text{Odd}.$$
$$\ddots$$
$$\kappa_1 s \tag{18}$$

Since $Q_N(s)$ is a Hurwitz polynomial, the coefficients $\kappa_i\ i = [1\ \ldots\ N]$ are all positive values and the rational functions in (18) are positive real (from Lemma 1). Next, we can also express the matrix $\boldsymbol{H}_a$ using a continued fraction expansion as

$$\boldsymbol{H}_a = \kappa_N \boldsymbol{a} + \left(\kappa_{N-1}\boldsymbol{b} + \left(\cdots + \left(\kappa_2 \boldsymbol{b} + (\kappa_1 \boldsymbol{a})^{-1}\right)^{-1}\right)^{-1}\right)^{-1}, \quad \text{if } N = \text{Even}$$

$$\boldsymbol{H}_a = \left(\kappa_N \boldsymbol{b} + \left(\kappa_{N-1}\boldsymbol{a} + \left(\cdots + \left(\kappa_2 \boldsymbol{b} + (\kappa_1 \boldsymbol{a})^{-1}\right)^{-1}\right)^{-1}\right)^{-1}\right)^{-1}, \quad \text{if } N = \text{Odd}. \tag{19}$$

The coefficients $\kappa_i\ i = [1\ \ldots\ N]$ in (19) are the same as in (18). Since $\mathbf{a}$ and $\mathbf{b}$ are positive-real matrices (due to the fact that the line parameters are nonnegative matrices [3], [6]), $\boldsymbol{H}_a$ in (19) is also positive real (from Lemmas 2 and 3).

Next, to prove that $\boldsymbol{H}_b$ is positive real, a similar strategy is followed. Let the rational function formed by $Q_{\mathrm{EV}}(s)$ and $Q_{\mathrm{ODD}}(s)$ be expressed as

$$\frac{Q_{\mathrm{ODD}}(s)}{Q_{\mathrm{EV}}(s)} = \kappa_N s + \cfrac{1}{\kappa_{N-1}s + \cfrac{1}{\kappa_{N-2}s + \cdots}} \qquad \text{if } N = \text{Odd}$$
$$\ddots$$
$$\kappa_1 s$$

$$\frac{Q_{\mathrm{ODD}}(s)}{Q_{\mathrm{EV}}(s)} = \cfrac{1}{\kappa_N s + \cfrac{1}{\kappa_{N-1}s + \cfrac{1}{\kappa_{N-2}s + \cdots}}} \qquad \text{if } N = \text{Even}.$$
$$\ddots$$
$$\kappa_1 s \tag{20}$$

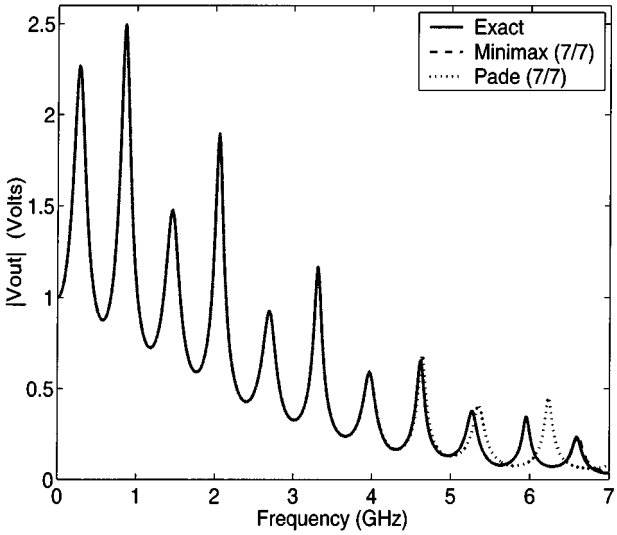

Fig. 3. Frequency response (Example 1).

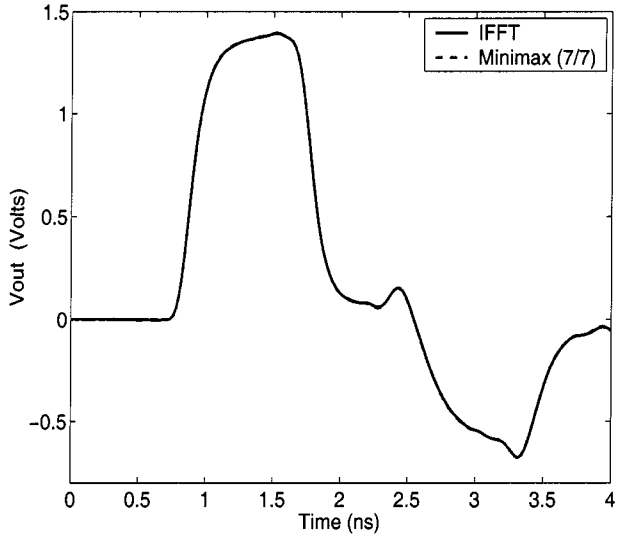

Fig. 4. Time-domain response (Example 1).

Since $Q_N(s)$ is a Hurwitz polynomial, the coefficients $\kappa_i\ i = [1\ \ldots\ N]$ are all positive values and the rational functions in

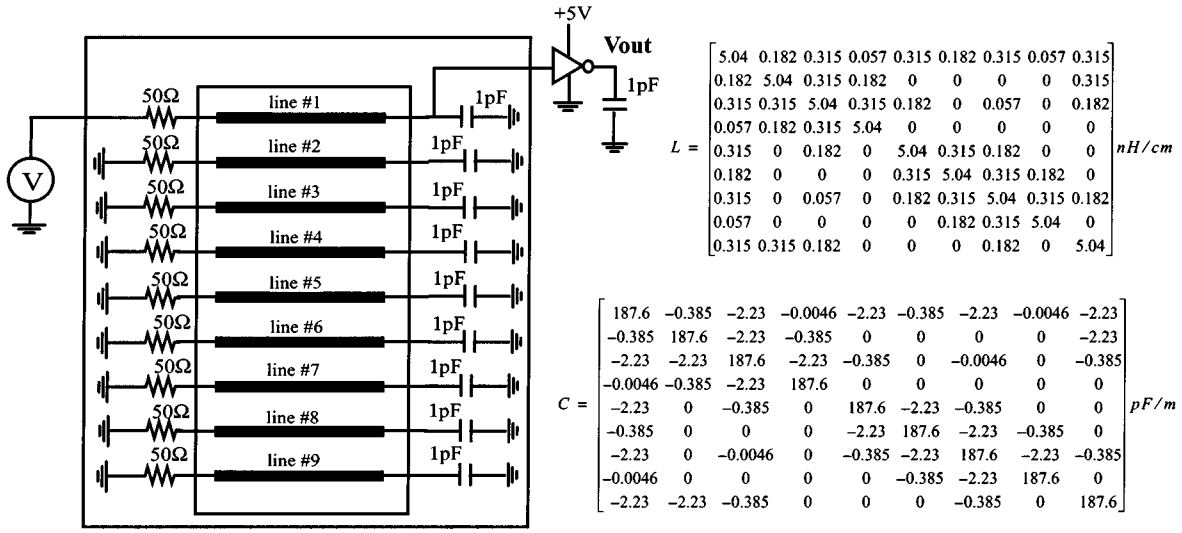

Fig. 5. Coupled interconnect system with nonlinear termination (Example 2).

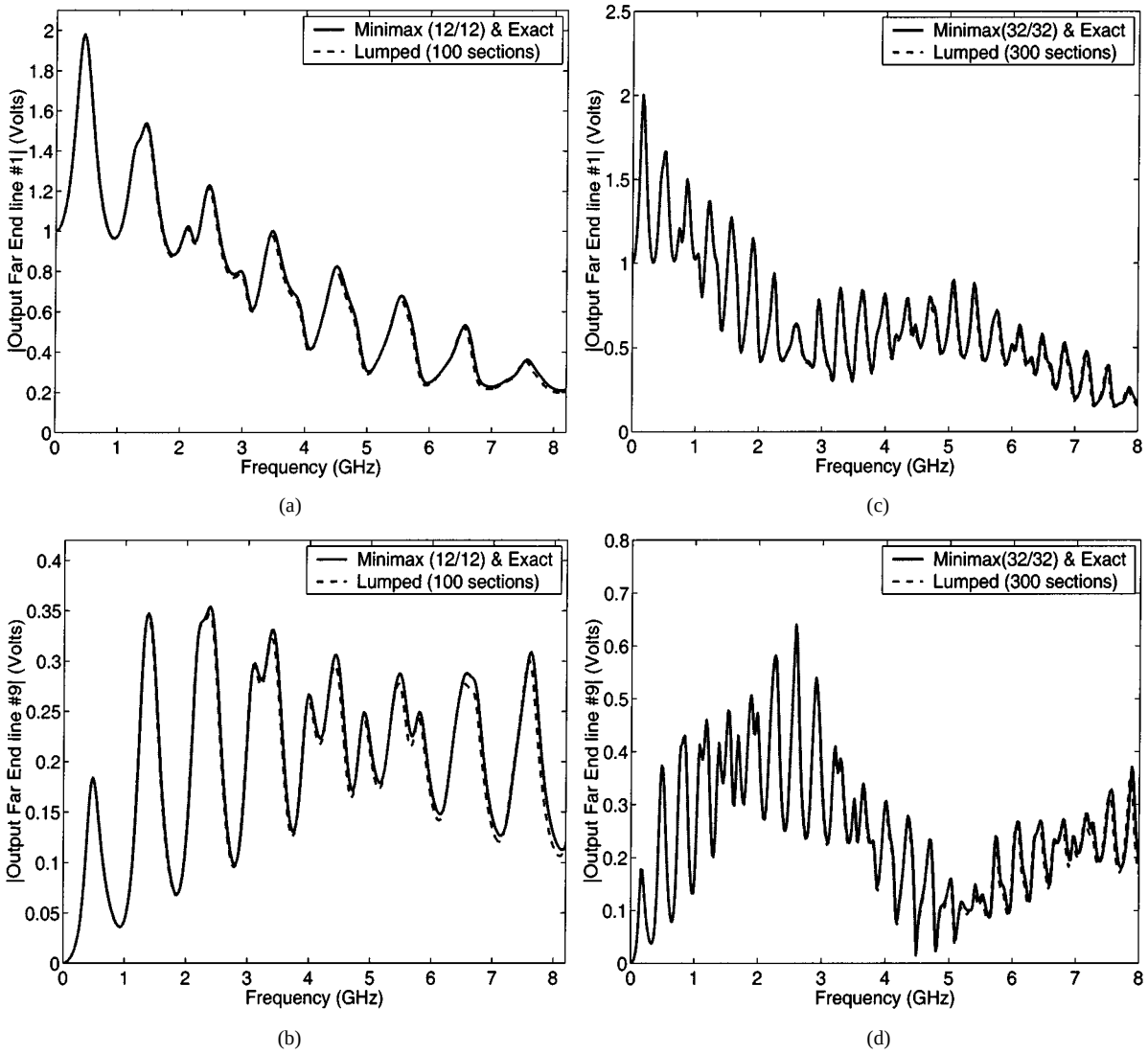

Fig. 6. Frequency response. (a) Far-end line 1 ($d = 5$ cm). (b) Far-end line 9 ($d = 5$ cm). (c) Far-end line 1 ($d = 15$ cm). (d) Far-end line 9 ($d = 15$ cm).

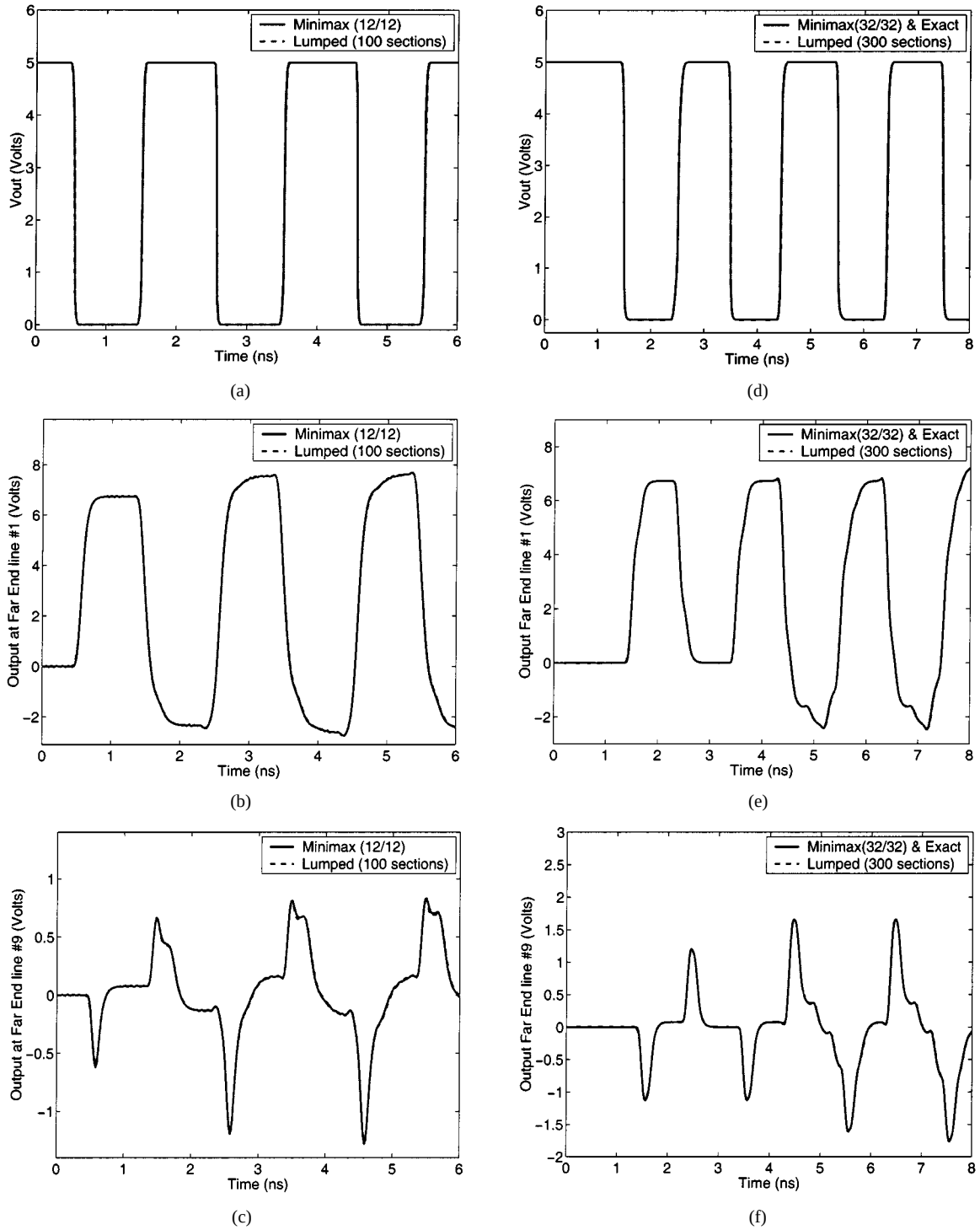

Fig. 7. Time-domain response. (a) Ouput of inverter ($d = 5$ cm). (b) Far-end line 1 ($d = 5$ cm). (c) Far-end line 9 ($d = 5$ cm). (d) Output of inverter ($d = 15$ cm). (e) Far-end line 1 ($d = 15$ cm). (f) Far-end line 9 ($d = 15$ cm).

(20) are positive real (from Lemma 1). Next, we can also express the matrix $\boldsymbol{H}_b$ using a continued fraction expansion as

$$\boldsymbol{H}_b = \kappa_N \boldsymbol{a} + \left(\kappa_{N-1}\boldsymbol{b} + \left(\cdots + \left(\kappa_2 \boldsymbol{a} + (\kappa_1 \boldsymbol{b})^{-1}\right)^{-1}\right)^{-1}\right)^{-1}, \quad \text{if } N = \text{Odd}$$

$$\boldsymbol{H}_b = \left(\kappa_N \boldsymbol{b} + \left(\kappa_{N-1}\boldsymbol{a} + \left(\cdots + \left(\kappa_2 \boldsymbol{a} + (\kappa_1 \boldsymbol{b})^{-1}\right)^{-1}\right)^{-1}\right)^{-1}\right)^{-1}, \quad \text{if } N = \text{Even}. \tag{21}$$

The coefficients κ_i $i = [1 \ \ldots \ N]$ in (21) are the same as in (20). Since $\mathbf{a}$ and $\mathbf{b}$ are positive-real matrices, $\boldsymbol{H}_b$ in (21) is also

TABLE I
PERFORMANCE COMPARISON (EXAMPLE 2)

Interconnect Length	Matrix-rational approximation		Conventional lumped segmentation		CPU Speed-up ratio
	# of poles	CPU time for transient analysis (seconds)	# of coupled sections	CPU time for transient analysis (seconds)	
5cm	216	73	100	336	4.6
15cm	576	301	300	2319	7.7

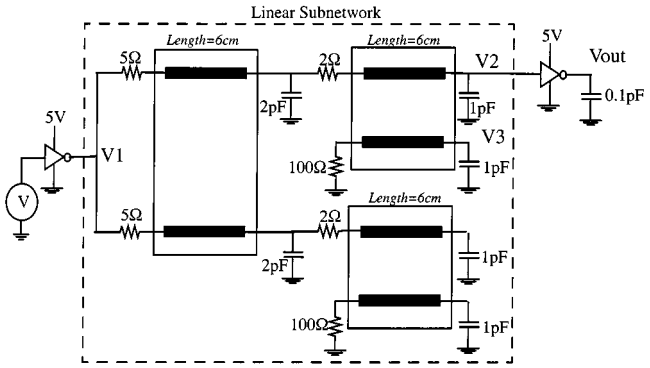

Fig. 8. Nonlinear circuit with frequency-dependent interconnect parameters (Example 3).

positive real (from Lemmas 2 and 3). This completes the proof of Theorem 1.

IV. CLASSES OF RATIONAL APPROXIMATIONS

Any rational-function approximation that satisfies the conditions of Theorem 1 can be used to obtain passive macromodels for transmission lines. In this section, we examine the existing passive rational approximations for exponential functions. In addition, we will present a technique to obtain near-optimal rational approximation for exponential functions.

A. Padé Rational Approximation

One method of obtaining the coefficients of (7) is to use a *Padé rational function.* The Padé coefficients of e^s can be obtained using the following closed-form relation [9]–[11], [25]:

$$e^s = \frac{\displaystyle\sum_{i=0}^{N} \frac{(M+N-i)!N!}{(M+N)!i!(N-i)!}\, s^i}{\displaystyle\sum_{i=0}^{M} \frac{(M+N-i)!M!}{(M+N)!i!(M-i)!}\,(-s)^i}. \tag{22}$$

For the case when M = N, the form of (22) is that of (7) and the Hurwitz condition is satisfied [26].

B. Minimax Rational Approximation

A compact expression for (7) can be obtained using a minimax approximation. The goal is to minimize the error function for a given interval such that

$$\max_{[f,\,g]} W(s)\left|e^s - \frac{q_N(s)}{p_M(s)}\right| \text{ is minimum} \tag{23}$$

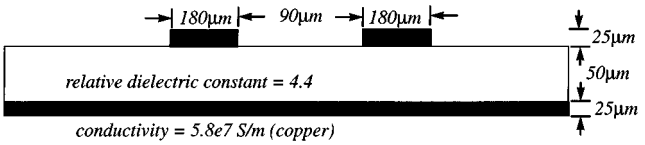

Fig. 9. Cross-sectional geometry and dimensions of microstrip (Example 3).

where $W(s)$ is a given weight function, $[f,\ g]$ is the interval of approximation, and $q_N(s)$ and $p_M(s)$ are the polynomials of the rational function of order M for the denominator and order N for the numerator.

Let the rational function of (7) be expressed in terms of products of factors written as

$$e^s \approx \frac{Q_N(s)}{Q_N(-s)} = \frac{\displaystyle\prod_{N=1}^{N/2}(s^2+\kappa_{1,N}s+\kappa_{0,N})}{\displaystyle\prod_{N=1}^{N/2}(s^2-\kappa_{1,N}s+\kappa_{0,N})}, \qquad N = \text{Even} \tag{24}$$

$$e^s \approx \frac{Q_N(s)}{Q_N(-s)} = \frac{(s+\kappa_{0,0})\displaystyle\prod_{N=1}^{(N-1)/2}(s^2+\kappa_{1,N}s+\kappa_{0,N})}{(-s+\kappa_{0,0})\displaystyle\prod_{N=1}^{(N-1)/2}(s^2-\kappa_{1,N}s+\kappa_{0,N})}, \qquad N = \text{Odd}. \tag{25}$$

Equations (24) and (25) satisfy the form of (7). Imposing the constraints that $\kappa_{0,N},\ \kappa_{1,N} > 0$ for all values of N ensures that $Q_N(s)$ is a strict Hurwitz polynomial. Replacing $s = j\omega$ and separating the rational function in terms of real and imaginary parts, the minimax objective function can be written as

$$\text{minmax}\left(\sum_{i=1}^{\chi}\left(W_{\text{re}}(\omega_i)\left(\cos\omega_i - \text{Re}\left(\frac{q_{N,N}(\omega_i)}{p_{N,N}(\omega_i)}\right)\right)^2 + W_{\text{im}}(\omega_i)\left(\sin\omega_i - \text{Im}\left(\frac{q_{N,N}(\omega_i)}{p_{N,N}(\omega_i)}\right)\right)^2\right)\right) \tag{26}$$

such that $\kappa_{0,N},\ \kappa_{1,N} > 0$ for all values of n. The variables $W_{\text{re}}(\omega_i)$, $W_{\text{im}}(\omega_i)$ are the weight functions at the angular frequency ω_i, where ω_i ranges from $f \le \omega_1 < \cdots < \omega_\chi \le g$;

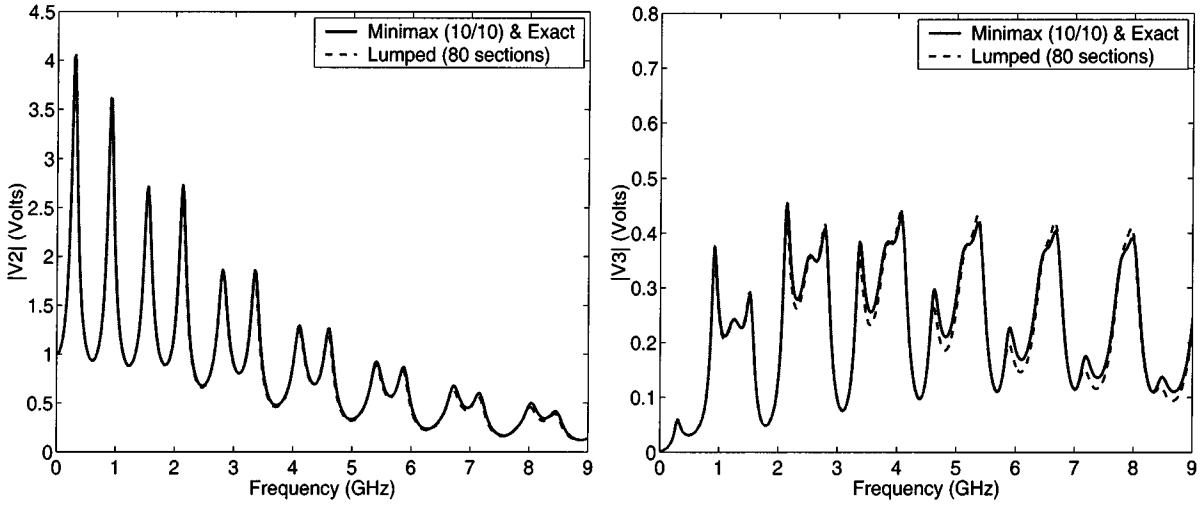

(a) (b)

Fig. 10. Frequency response: (a) at node V2 and (b) at node V3.

TABLE II
PER-UNIT-LENGTH PARAMETERS (EXAMPLE 3)

F(GHz)	1e-5	1e-4	1.1e-3	1.1e-2	0.12	0.38	0.76	1.21	1.94	2.45	3.10	3.91	4.95	6.26	7.91	10.0
R_{11}(Ω/m)	4.63	4.75	5.24	6.47	15.6	28.1	39.9	50.5	63.8	71.7	80.6	90.6	102	115	129	145
R_{12}(Ω/m)	0.74	0.76	0.55	0.44	1.48	2.72	3.88	4.90	6.18	6.94	7.80	8.75	9.83	11.0	12.4	13.9
L_{11}(nH/m)	337	335	285	230	209	203	200	199	197	197	196	195	195	195	194	194
L_{12}(nH/m)	58.4	57.2	13.1	17.2	15.0	14.4	14.1	13.9	13.8	13.7	13.7	13.6	13.6	13.6	13.5	13.5

$$C = \begin{bmatrix} 193 & -1.53 \\ -1.53 & 193 \end{bmatrix} \frac{pF}{m} \qquad G = \begin{bmatrix} 0 & 0 \\ 0 & 0 \end{bmatrix} \frac{S}{m}$$

$$R_{11} = R_{22} \quad R_{12} = R_{21} \qquad L_{11} = L_{22} \quad L_{12} = L_{21}$$

$\mathrm{Re}(\,)$, $\mathrm{Im}(\,)$ are the real and imaginary parts of the rational function.

The results obtained by the minimax approximation for various orders and frequency ranges are then stored. Thus, the macromodel can be formed analytically in terms of stored (predetermined) constants and the per-unit-length parameters.

V. DEVELOPMENT OF THE TIME-DOMAIN MACROMODEL

In this section, we will briefly review the technique to realize the macromodel of (5) in terms of ordinary differential equations [9]–[11]. The rational matrix of (8) can be represented in terms of products of subsections described by the poles and zeros of e^s as follows:

$$\begin{aligned}\Big[\boldsymbol{Q}_N(-\boldsymbol{Z})\Big]^{-1}\boldsymbol{Q}_N(\boldsymbol{Z}) &= \prod_{i=1}^{N/2}\Big[\boldsymbol{Q}_N(-\boldsymbol{Z})_i\Big]^{-1}\Big[\boldsymbol{Q}_N(\boldsymbol{Z})_i\Big] \\ &= \prod_{i=1}^{N/2}\Big[(a_i\boldsymbol{U}-\boldsymbol{Z})(a_i^*\boldsymbol{U}-\boldsymbol{Z})\Big]^{-1}\Big[(a_i\boldsymbol{U}+\boldsymbol{Z})(a_i^*\boldsymbol{U}+\boldsymbol{Z})\Big]\end{aligned} \tag{27}$$

for even values of n, and

$$\begin{aligned}&\Big[\boldsymbol{Q}_N(\boldsymbol{Z})\Big]^{-1}\boldsymbol{Q}_N(\boldsymbol{Z}) \\ &\quad= \prod_{i=0}^{(N-1)/2}\Big[\boldsymbol{Q}_N(\boldsymbol{Z})_i\Big]^{-1}\Big[\boldsymbol{Q}_N(\boldsymbol{Z})_i\Big] \\ &\quad= \Big[a_0\boldsymbol{U}-\boldsymbol{Z}\Big]^{-1}\Big[a_0\boldsymbol{U}+\boldsymbol{Z}\Big]\prod_{i=1}^{(N-1)/2}\Big[(a_i\boldsymbol{U}-\boldsymbol{Z}) \\ &\qquad\qquad\cdot(a_i^*\boldsymbol{U}-\boldsymbol{Z})\Big]^{-1} \\ &\qquad\cdot\Big[(a_i\boldsymbol{U}+\boldsymbol{Z})(a_i^*\boldsymbol{U}+\boldsymbol{Z})\Big]\end{aligned} \tag{28}$$

for odd values of N. Here, $\boldsymbol{U}$ represents the unity matrix and $a_i = x_i + jy_i$ are complex roots for $i > 0$, and a_0 is a real root. The symbol $*$ represents the complex conjugate operation. Converting each subsection i to the Y-parameters yields

$$\begin{aligned}\boldsymbol{Y}_{11} &= \boldsymbol{Y}_{22} \\ &= \frac{\rho_i^2}{4x_id}\big(\boldsymbol{a}(s)\big)^{-1} + \frac{\boldsymbol{b}(s)d}{4x_i} + x_i\left(\boldsymbol{a}(s)d + \frac{\rho_i^2}{d}\big(\boldsymbol{b}(s)\big)^{-1}\right)^{-1} \\ \boldsymbol{Y}_{12} &= \boldsymbol{Y}_{21} \\ &= \frac{\rho_i^2}{4x_id}\big(\boldsymbol{a}(s)\big)^{-1} + \frac{\boldsymbol{b}(s)d}{4x_i} - x_i\left(\boldsymbol{a}(s)d + \frac{\rho_i^2}{d}\big(\boldsymbol{b}(s)\big)^{-1}\right)^{-1}\end{aligned} \tag{29}$$

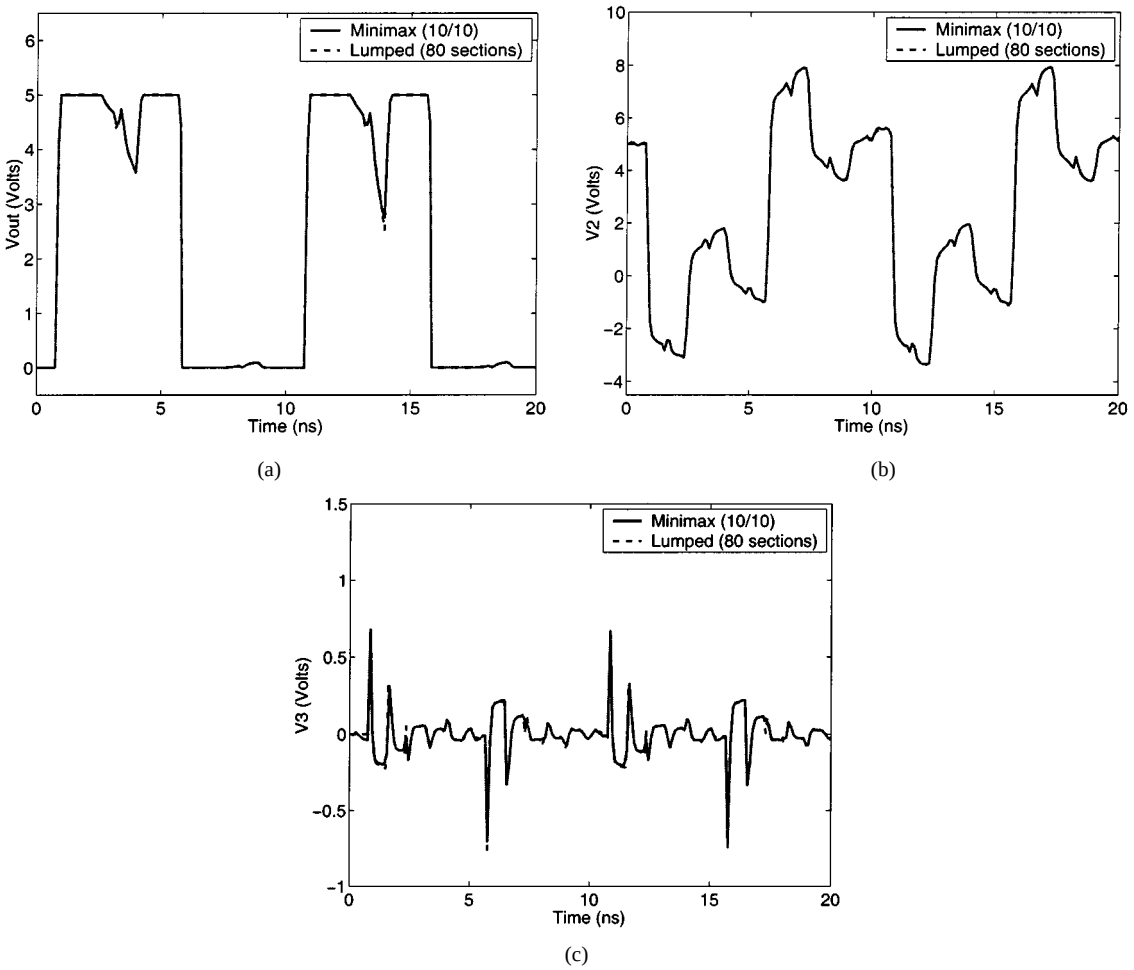

Fig. 11. Time-domain response: (a) at node Vout (output of inverter), (b) at node V2, and (c) at node V3.

for the complex pole-zero subsection and

$$\boldsymbol{Y}_{11} = \boldsymbol{Y}_{22} = \frac{a_0}{2d}\left(\boldsymbol{a}(s)\right)^{-1} + \frac{d}{2a_0}\left(\boldsymbol{b}(s)\right)$$
$$\boldsymbol{Y}_{12} = \boldsymbol{Y}_{21} = -\frac{a_0}{2d}\left(\boldsymbol{a}(s)\right)^{-1} + \frac{d}{2a_0}\left(\boldsymbol{b}(s)\right) \qquad (30)$$

for the real pole subsection, where $\rho_i^2 = x_i^2 + y_i^2$.

Since (29) and (30) is in the form of ration function, it can be easily translated analytically to a set of ordinary differential equations using similar techniques reported in [9]–[11].

A. Criteria for Selecting the Order of Approximation

Accuracy of the proposed model depends on the order of the approximation (N, M). Since all the elements in (10) are computed using the predetermined coefficients and in a closed-form manner, the required order (N, M) can be easily estimated using the following error criterion:

$$\left\| e^{\boldsymbol{Z}} - \left(\boldsymbol{P}_{N,M}^{-1}(\boldsymbol{Z})\boldsymbol{Q}_{N,M}(\boldsymbol{Z})\right)\right\| < \varepsilon \qquad (31)$$

where ε is the predefined error tolerance. If the error tolerance is not satisfied over the frequency range of interest, the order of the macromodel can be increased.

VI. Computational Results

Example 1: The coupled interconnect configuration proposed in [18] is shown in Fig. 2. The frequency response obtained using the minimax and Padé macromodels (order 7/7) are compared with the direct solution of telegrapher's equations (here onwards referred by the term "exact") in Fig. 3. The Padé approximation deviates from the exact response after 4 GHz, while the minimax approximation deviates after 6 GHz. To achieve the same frequency accuracy as the minimax approximation, order 10/10 is required by the Padé approximation. The transient response corresponding to an input pulse with 0.1-ns rise/fall times and a 0.8-ns pulsewidth is shown in Fig. 4. Both the minimax approximation and inverse fast Fourier transform (IFFT) response match.

Example 2: A distributed interconnect network with nine coupled lines (Fig. 5) is analyzed using the proposed technique. Two different cases of interconnect length d are considered, i.e., 5 and 15 cm. The frequency response of the linear subnetwork is matched up to 8 GHz using the proposed method

and lumped model. A comparison of sample frequency response corresponding to signal and victim lines is given in Fig. 6. As seen, the response obtained using the proposed approach is indistinguishable from the exact response. The transient response of the entire nonlinear network for a trapezoidal input pulse with a 0.1-ns rise/fall time, 0.8-ns pulsewidth, and a 2-ns period is shown in Fig. 7. The efficiency of the proposed method is shown in Table I. It is to be noted that, the savings achieved using the proposed macromodel is higher for longer lines and if the macromodels are to match larger bandwidths.

Example 3: A distributed interconnect network with frequency-dependent parameters is considered in Fig. 8. The interconnect dimensions are shown in Fig. 9. The corresponding per-unit-length parameters were computed using OPTEMID[1] and are listed in Table II. The values of $\mathbb{R}$ and $\mathbb{L}$ were fitted to a positive-real rational matrix, as described in [10]. The frequency response of the linear subnetwork (Fig. 10) is obtained by applying a voltage source at node V1. The proposed method (order 10/10) matches the exact frequency response up to 9 GHz. Fig. 11 shows the transient response of the entire nonlinear circuit corresponding to a 5-V trapezoidal input pulse with 0.1-ns rise/fall times, 4.8-ns pulsewidth, and a 10-ns period.

VII. Conclusions

In this paper, a general class of passive macromodeling algorithm for multiport distributed interconnects has been presented. The proposed approach is based on matrix-rational approximation of exponential functions describing the Telegrapher's equations. A new theorem is described that specifies the necessary conditions for any matrix-rational approximation of exponential functions in order to generate a passive macromodel. In addition, a technique to obtain very compact passive macromodel with predetermined coefficients, based on near-optimal approximation, has been presented. The proposed model can be easily incorporated with the recently developed passive model-reduction techniques.

References

[1] A. Deustsch, "Electrical characteristics of interconnections for high-performance systems," *Proc. IEEE*, vol. 86, pp. 315–355, Feb. 1998.

[2] A. Deutch *et al.*, "When are transmission-line effects important for on-chip interconnections?," *IEEE Trans. Microwave Theory Tech.*, vol. 45, pp. 1836–1846, Oct. 1997.

[3] C. R. Paul, *Analysis of Multiconductor Transmission Lines*. New York, NY: Wiley, 1994.

[4] R. Achar and M. Nakhla, "Simulation of high-speed interconnects," *Proc. IEEE*, vol. 89, pp. 693–728, May 2001.

[5] High-speed circuit and interconnect analysis I and II, Multimedia learning course [Online]. Available: http: //www.omniz.com.

[6] F. Y. Chang, "The generalized method of characteristics for wave-form relaxation analysis of coupled transmission lines," *IEEE Trans. Microwave Theory Tech.*, vol. 37, pp. 2028–2038, Dec. 1989.

[7] M. Celik, A. C. Cangellaris, and A. Yaghmour, "An all purpose transmission line model for interconnect simulation in SPICE," *IEEE Trans. Microwave Theory Tech.*, vol. 45, pp. 127–138, Oct. 1997.

[8] A. C. Cangellaris, S. Pasha, J. L. Prince, and M. Celik, "A new discrete time-domain model for passive model order reduction and macromodeling of high-speed interconnections," *IEEE Trans. Comp. Packag. Technol.*, pp. 356–364, Aug. 1999.

[9] A. Dounavis, X. Li, M. Nakhla, and R. Achar, "Passive closed-loop transmission line model for general purpose circuit simulators," *IEEE Trans. Microwave Theory Tech.*, vol. 47, pp. 2450–2459, Dec. 1999.

[10] A. Dounavis, R. Achar, and M. Nakhla, "Efficient passive circuit models for distributed networks with frequency-dependent parameters," *IEEE Trans. Adv. Packag.*, vol. 23, pp. 382–392, Aug. 2000.

[11] A. Dounavis, E. Gad, R. Achar, and M. Nakhla, "Passive model reduction of multiport distributed interconnects," *IEEE Trans. Microwave Theory Tech.*, vol. 48, pp. 2325–2334, Dec. 2000.

[12] W. T. Beyene and J. E. Schutt-Ainé, "Efficient transient simulation of high-speed interconnects characterized by sampled data," *IEEE Trans. Comps., Packag., Manuf. Technol.*, pt. B, vol. 21, pp. 105–113, Feb. 1998.

[13] L. T. Pillage and R. A. Rohrer, "Asymptotic waveform evaluation for timing analysis," *IEEE Trans. Computer-Aided Design*, vol. 9, pp. 352–366, Apr. 1990.

[14] P. Feldmann and R. W. Freund, "Efficient linear circuit analysis by Padé approximation via Lanczos process," *IEEE Trans. Computer-Aided Design*, vol. 14, pp. 639–649, May 1995.

[15] L. M. Silviera, M. Kamen, I. Elfadel, and J. White, "A coordinate transformed Arnoldi algorithm for generating guaranteed stable reduced-order models for *RLC* circuits," in *ICCAD Tech. Dig.*, Nov. 1996, pp. 2288–2294.

[16] E. Chiporout and M. S. Nakhla, "Analysis of interconnect networks using complex frequency hopping," *IEEE Trans. Computer-Aided Design*, vol. 14, pp. 186–199, Feb. 1995.

[17] M. Celik and A. C. Cangellaris, "Simulation of dispersive multiconductor transmission lines by Padé via Lanczos process," *IEEE Trans. Microwave Theory Tech.*, vol. 44, pp. 2525–2535, Dec. 1996.

[18] ——, "Efficient transient simulation of lossy packaging interconnects using moment-matching techniques," *IEEE Trans. Comp., Packag. Manufact. Technol. B*, vol. 19, pp. 64–73, Feb. 1996.

[19] A. Odabasioglu, M. Celik, and L. T. Pilleggi, "PRIMA: Passive reduced-order interconnect macromodeling algorithm," *IEEE Trans. Computer-Aided Design*, vol. 17, no. 8, pp. 645–654, Aug. 1998.

[20] Q. Yu, J. L. Wang, and E. Kuh, "Passive multipoint moment matching model order reduction algorithm on multiport distributed interconnect networks," *IEEE Trans. Circuits Syst. I*, vol. 46, pp. 140–160, Jan. 1999.

[21] A. Dounavis, R. Achar, and M. Nakla, "Efficient sensitivity analysis of lossy multiconductor transmission lines with nonlinear terminations," *IEEE Trans. Microwave Theory Tech.*, to be published.

[22] E. S. Kuh and R. A. Rohrer, *Theory of Linear Active Networks*. San Francisco, CA: Holden-Day, 1967.

[23] D. F. Tuttle, *Electrical Networks; Analysis and Synthesis*. New York: McGraw-Hill, 1965.

[24] R. W. Newcomb, *Linear Multiport Synthesis*. New York: McGraw-Hill, 1966.

[25] J. Vlach and K. Singhal, *Computer Methods for Circuit Analysis and Design*. New York: Van Nostrand, 1983.

[26] U. S. Pillai, *Spectrum Estimation and System Identification*. Berlin, Germany: Springer-Verlag, 1993.

[1]Version 4.3, OPTEM Engineering Inc., Calagary, AB, Canada.

Anestis Dounavis (S'99) received the B.Eng. degree from McGill University, Montreal, QC, Canada, in 1995, the M.Eng. degree from Carleton University, Ottawa, ON, Canada, in 2000, and is currently working toward the Ph.D. degree in electronics at Carleton University.

His research interests includes modeling and simulation of high-speed interconnects, computer-aided design of very large scale integration (VLSI) systems, and numerical algorithms.

Mr. Dounavis was the recipient of the Carleton University Medal for his M.Eng. degree thesis on time-domain macromodeling of high-speed interconnects.

Ramachandra Achar (S'95–M'99) received the B.Eng. degree in electronics engineering from Bangalore University, Banglaore, India, in 1990, the M.Eng. degree in microelectronics from the Birla Institute of Technology and Science, Pilani, India, in 1992 , and the Ph.D. degree from Carleton University, Ottawa, ON, Canada, in 1998.

In the summer of 1995, he was with the T. J. Watson Research Center, IBM, New York, NY, where he was involved with high-speed interconnect analysis. In 1992, he was a Graduate Trainee at the Central Electronics Engineering Research Institute, Pilani, India, and was also previously with Larsen and Toubro Engineers Ltd., Mysore, India and the Indian Institute of Science, Bangalore, India, as a Research and Development Engineer. From 1998 to 2000, he was a Research Engineer in the Computer-Aided Engineering Group at Carleton University. His research interests include modeling and simulation of high-speed interconnects, numerical algorithms, and development of computer-aided design tools for high-frequency circuit analysis. He is currently an Assistant Professor in the Department of Electronics, Carleton University.

Dr. Achar was the recipient of several prestigious awards, including the 2000 Natural Science and Engineering Research Council Doctoral Award, the 1997 Strategic Microelectronics Corporation Award, the 1996 Canadian Microelectronics Corporation Award, and the 1998 Best Student Paper Award presented at the Micronet (a Canadian network of centers of excellence on Microelectronics) Annual Workshop. He was also the recipient of the Carleton University Medal for his doctoral work on high-speed VLSI interconnect analysis.

Michel Nakhla (S'73–M'75–SM'88–F'98) received the M.A.Sc. and Ph.D. degrees in electrical engineering from the University of Waterloo, Waterloo, ON, Canada, in 1973 and 1975, respectively.

From 1976 to 1988, he was the Senior Manager of the Computer-Aided Engineering Group with Bell-Northern Research, Ottawa, ON, Canada. In 1988, he joined Carleton University, as a Professor and the Holder of the Computer-Aided Engineering Senior Industrial Chair established by Nortel Networks and the Natural Sciences and Engineering Research Council of Canada. He is currently a Professor of electrical engineering at Carleton University. He is the founder of the high-speed Computer-Aided Design (CAD) Research Group at Carleton University, and is a frequent invited speaker on the topic of high-speed interconnects. He is a technical consultant for several industrial organizations and is the principal investigator for several major sponsored research projects. His research interests include CAD of VLSI and microwave circuits, modeling and simulation of high-speed interconnects, nonlinear circuits, multidisciplinary optimization, thermal and electromagnetic (EM) emission analysis, microelectromechanical systems (MEMS), and neural networks.